



1

2

3 **Ozone and temperature decadal solar-cycle responses, and their relation to diurnal**  
4 **variations in the stratosphere, mesosphere, and lower thermosphere, based on**  
5 **measurements from SABER on TIMED.**

6

7 **Frank T. Huang<sup>1\*</sup>, Hans G. Mayr<sup>2\*</sup>**

8 <sup>1</sup>University of Maryland, Baltimore County, MD 21250, USA

9 <sup>2</sup>NASA Goddard Space Flight Center, Greenbelt, MD 20771, USA

10 \*retired

11

12 **Abstract.** There is evidence that the ozone and temperature responses to the solar cycle of ~11  
13 years depend on the local times of measurements. Here we present relevant results based on  
14 SABER data over a full diurnal cycle, not available previously. In this area, almost all satellite  
15 data used are made at only one or two fixed local times, which can be different among various  
16 satellites. Consequently, estimates of responses can be different depending on the specific data  
17 set. Also, over years, due to orbital drift, the local times of measurements of some satellites have  
18 also drifted. In contrast, SABER makes measurements at various local times, providing the  
19 opportunity to estimate diurnal variations over 24 hrs. We can then also estimate responses to the  
20 solar cycle over both a diurnal cycle and at the fixed local times of specific satellite data for  
21 comparison. Our results of responses, based on zonal means of SABER measurements, agree  
22 favorably with previous studies based on data from the HALOE instrument, which measured  
23 data only at sunrise and sunset, thereby supporting the analysis of both studies. We find that for  
24 ozone above ~ 40km, zonal means reflecting specific local times (e.g., 6, 12, 18, 24 hrs) lead to  
25 different values of responses, and to different responses based on zonal means that are also  
26 averages over the 24 hours of local time, as in 3D models. For temperature, effects of diurnal  
27 variations on the responses are not negligible even at ~30 km and above. We also have  
28 considered the consequences of local-time variations due to orbital drifts of certain operational  
29 satellites, and for both ozone and temperature, their effects can be significant above ~30 km.  
30 Previous studies based other satellite data do not describe their treatment, if any, of local times.  
31 Some studies also analyzed data merged from different sources, with measurements made at  
32 different local times. Generally, the results of these studies do not agree so well among  
33 themselves. Although responses are a function of diurnal variations, this is not to say that they  
34 are the major reason for the differences, as there are likely other data-related issues. The effects  
35 due to satellite orbital drift may explain some unexpected variations in the responses, especially  
36 above 40 km.

37

38 **1.0 Introduction**

39 The response of atmospheric ozone and temperature to the solar cycle of ~11 years is  
40 important for both scientific and practical reasons. Global responses in the stratosphere,  
41 mesosphere, and lower thermosphere have been investigated over decades based on a variety of  
42 satellite data.

43 There is evidence that the values of the responses to decadal solar cycles depend on the local  
44 times at which the measurements are made.

45 However, with few exceptions, the instruments on satellites measure at only one or two local  
46 times, which are fixed for the entire mission.



47 Generally, previous studies do not address in detail the issue of diurnal variations of the  
48 responses, and there have been no studies describing their variations over the 24 hrs of local  
49 time. In the following, we provide estimates of the diurnal variations of the responses over a 24  
50 hrs, which has not been available previously.

51 As noted in Huang et al. [2016b], previous global empirical results have been largely based  
52 on data from the NOAA operational satellites (which include the Stratosphere Sounding Unit  
53 (SSU), the Microwave Sounding Unit (MSU), and the Solar Backscatter Ultraviolet (SBUV)  
54 instruments), from the Stratospheric Aerosol and Gas Experiment (SAGE I, II), on the Explorer  
55 and Earth Radiation Budget (ERB) satellites, from the Halogen Occultation Experiment  
56 (HALOE) on the Upper Atmosphere Research Satellite (UARS), and from the Sounding of the  
57 Atmosphere using Broadband Emission Radiometry (SABER) instrument on the Thermosphere-  
58 Ionosphere-Mesosphere-Energetics and Dynamics (TIMED) satellite, among others. The  
59 advantage of the operational satellites is that they can provide global measurements covering  
60 decades, being replaced as needed. However, issues of instrument offsets, stability, and  
61 continuity over many years and decades can be problematic.

62 Except for SABER (and UARS), instruments on these satellites make measurements at only  
63 one or two local times, which are fixed for the mission duration. The NOAA operational  
64 satellites are sun-synchronous, in which case the measurements are made at two fixed local  
65 times, one for the ascending orbital mode, and one for the descending mode. HALOE and SAGE  
66 make solar occultation measurements, only at instrument sunrise and sunset. Consequently, used  
67 as is, responses based on zonal means of the above measurements reflect long term variations at  
68 the fixed local times, and could be a source of differences among the various studies.

69 They could also be a source of differences with 3D models, whose ozone amounts and  
70 temperature vary with local time around a latitude circle, and whose zonal means are averages  
71 over both longitude and 24 hrs of local time. When comparing results of responses based on  
72 zonal means from measurements with models, Austin et al. [2008] point out that “The model  
73 results are strictly zonal average values, which is an average over local time, whereas the  
74 observations are typically made at fixed local times. Therefore, in the mesosphere, where the  
75 diurnal variation of ozone is large, some of the differences between model results and  
76 observations may have arisen from a diurnal variation in the actual solar response”. See also  
77 Beig et al. [2012].

78 In addition, the orbits of some operational satellites have drifted, so that the local times at  
79 which the measurements are made have also drifted over several hours or more (see McPeters et  
80 al. [2013], Frith et al. [2014], Remsberg [2008], Randel et al. [2009], Tummon et al. [2015],  
81 Hood et al. [2015]). Tumman et al. [2015] summarizes some of the data processing methods  
82 taken by various groups. Generally, they report that diurnal variations are either neglected, or are  
83 assumed to be negligible below ~ 45-50 km. See also Davis et al. (2015).

84 Previous results have not generally agreed so well with one another in their details. A major  
85 reason for these differences may be the conditions and constraints under which the various  
86 measurements were made (Austin et al., 2008, Crooks and Gray [2005], Gray et al. [2005],  
87 Huang et al. [2016b]).

88 In addition, previous studies generally have not described how they treat diurnal variations, so  
89 that comparisons related to responses as a function of local times are problematical. We are also  
90 not aware of studies based on orbital drift.

91 In contrast to most other measurements, SABER provide additional information which allows  
92 us to estimate daily ozone and temperature diurnal variations, and then also the dependence of



93 their responses to the decadal solar cycle on local time. In the following, we focus on zonal  
94 means of ozone and temperature, either at various specific local times, or averaged over local  
95 times (as in 3D model), and the effects of their diurnal variations on their responses to solar  
96 variability over a solar cycle of ~11 years (2002-2014), from 20 to 100 km.

97 In this study, we find that not only do the values of the responses depend on the local times at  
98 which the measurements are made, but they can be significant even at altitudes as low as 30 km.

99 In Section 2, we review our previous analysis and derivation of diurnal variations and zonal  
100 means that are averages of both longitude and local time around a latitude circle, based on  
101 SABER measurements. We also describe how we can estimate new results of zonal means  
102 corresponding to specific local times, and new results in estimating effects of orbital drift on  
103 diurnal variations.

104 In Section 3 we describe our new results of responses to the solar cycle at the specific local  
105 times of sunrise (6hrs) and sunset (18hrs), and compare with results from HALOE. This gives an  
106 indication of the quality and reality of our and HALOE's results.

107 In Section 4 we describe our new results of responses to the solar cycle over a diurnal cycle of  
108 24 hrs.

109 In Section 5 we describe our estimates of responses in situations where the local times have  
110 'drifted' due to satellite orbital drifts. We also describe some previous studies.

111 In Section 6 we discuss the issue of data length.

112

## 113 **2.0 SABER analysis.**

114 The data are provided by the SABER project (version 2.0, level2A). They are interpolated to 4-  
115 degree latitude and 2.5 km altitude grids, after which zonal averages are taken for analysis.

116 In contrast to other satellite measurements, those from SABER (Russell et al., 1999) contain  
117 information to estimate the diurnal variations of ozone and temperature, and the results are  
118 described in Huang et al. [2010a, 2010b].

119 As noted in Huang et al. [2016b], SABER ozone and temperature measurements have been  
120 analyzed with success for more than a decade. We have derived variations with periods from one  
121 day or less (diurnal variations) up to multiple years (semiannual oscillations (SAO) and quasi-  
122 biennial oscillations (QBO)), and one decade or more (trends, responses to solar cycle). See  
123 Huang et al. [2008a,b, 2010a,b, 2014, 2016a,b]. Zhang et al. [2006] and Mukhtarov et al. [2009]  
124 have derived temperature diurnal tides using SABER data, and Nath and Sridharan [2014] have  
125 also derived responses to solar variability using SABER data.

126 For both ozone and temperature, these studies show that, for variations that are deviations from  
127 a mean state (e.g., diurnal variations, tides, semiannual and quasi-biennial oscillations, responses  
128 to solar variability, trends), SABER measurements are robust and precise. For example, zonal  
129 mean tidal temperatures can agree with other measurements to within ~ 1°K (Huang et al.,  
130 2010a), and our zonal mean ozone diurnal variations can agree with other diurnal measurements  
131 to less than a few percent (Huang et al., 2010b).

132 These previous results contain

- 133 1) diurnal variations of ozone and temperature for each day of the year, and
- 134 2) zonal means that are averages over both longitude and local time in a consistent manner,  
135 which can then be compared directly with 3D models.

136

137 Using these, we can then estimate the goals of this study, which is to

- 138 3) reconstruct the zonal means to reflect specific local times.



139 4) calculate responses to solar variability over a solar cycle at specific local times  
140 5) estimate local time variations of responses as a result of orbital drifts of NOAA satellites,  
141 as noted above.

142 We can therefore find the variation of responses to the solar cycle over the 24hrs of local time,  
143 including at 6 and 18hrs for comparison with responses based on HALOE data at sunrise and  
144 sunset for comparison (see Beig et al. [2012], Fadnavis and Beig [2006]).

145 Compared to the stratosphere, diurnal variations of ozone and temperature themselves are  
146 more prominent in the mesosphere and lower thermosphere. Even in the stratosphere, they may  
147 not be negligible (Huang et al. 2010a, 2010b). Between ~30 and 80 km, ozone diurnal variations  
148 are due mainly to photochemistry (Brasseur and Solomon, 2005), while temperature diurnal  
149 variations are mainly a result of thermal tides (Chapman and Lindzen, 1970). For diurnal  
150 variations, our results for both ozone and temperature (Huang et al. 2010a, 2010b) show that they  
151 can be systematic from the lower thermosphere down to 25 km. This is consistent with results by  
152 Sakazaki et al. [2015] for ozone, and Oberheide et al.[2000] and Gille et al. [1991] for  
153 temperature.

154 As discussed below, for responses to the solar cycle, our results show that the effects of local  
155 time variations can be non-negligible for altitudes even below 40 km, especially for temperature.

156

## 157 **2.1 Previous analysis**

158

### 159 **2.1.1 Diurnal variations**

160 As noted in Huang et al. [2016b], unlike other satellites mentioned above (except UARS), the  
161 orbital characteristics of TIMED are such that SABER samples over the 24 hrs of local time,  
162 which can be used to estimate diurnal variations of ozone and temperature. A complication is  
163 that it takes SABER 60 days to sample over the 24 hrs of local time. Over 60 days, the variations  
164 with local time are embedded with the seasonal variations, and need to be separated from them.  
165 The method we use estimates both the diurnal and mean variations (e.g., seasonal, semiannual,  
166 annual) together, by performing a least squares fit of a two-dimensional Fourier series, where the  
167 independent variables are local time and day of year. The algorithm is discussed further in Huang  
168 et al. [2010a,b].

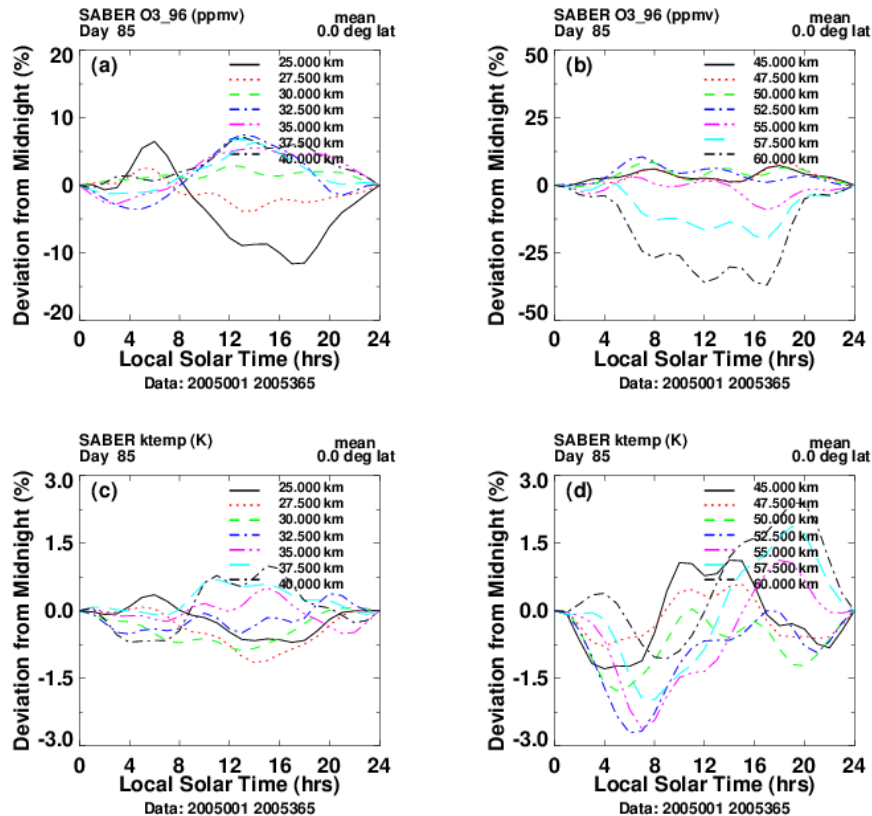
169 The top row of Figure 1 shows zonal mean ozone diurnal variations (percent deviation from  
170 midnight) for day 85 of 2005, at the equator, from 25 to 40 km (left panel), 45 to 60 km (right  
171 panel), based on SABER data. See Huang et al. [2010b] for details. It can be seen that diurnal  
172 variations can be significant even at 25 km.

173 The bottom row of Figure 1 corresponds to the top row, but for temperature. See Huang et al.  
174 [2010a] for details. Even at altitudes near 30 km, the diurnal variations are systematic and, as  
175 seen below, can affect results in estimating decadal responses. Although small, at 30 km, the  
176 diurnal variations of temperature compare well with Zeng et al. [2008], Oberheide et al.[2000],  
177 Gille et al.[1991], based on different types of measurements.

178

179

180



181  
 182 **Figure 1.** Top row: ozone zonal mean mixing ratios (ppmv) versus local time for day 05085 at the Equator. Left  
 183 panel (a): 25 to 40 km (percent deviation from midnight), right panel (b): 45 to 60 km. Bottom row: as in top row,  
 184 but for temperature (K).

185  
 186 **2.1.2 Mean variations.**

187 Once the diurnal variations are known for each day, the zonal mean variations, which are  
 188 averages over longitude and local time, consistent with 3D models, can be obtained.

189 Based on these zonal means, our results of decadal responses to solar activity, as represented  
 190 by the 10.7 cm solar flux, had been presented in Huang et al. [2016a, 2016b].

191  
 192 **2.2 Current analysis**

193 For the current study, we generate

194 a) monthly zonal means that are averaged over longitude, but at specific local times. These  
 195 correspond to those satellite measurements which sample at specific local times

196 b) zonal means with local times that vary from month to month, to simulate the situation  
 197 caused by satellite orbital drifts, as described earlier.

198 c) estimates of responses to solar the cycle, based on a) and b), and compare with responses  
 199 based on zonal means that are also averaged over local time.

200 As an example, in Figure 2, the left panel (a) shows our ozone monthly mean mixing ratios  
 201 (red line, parts per million by volume, ppmv) at 47.5 km and the Equator, from mid 2002 to mid



202 2014, with seasonal and local time variations removed. The green line represents how the data  
 203 would vary if we simulated the variations with local time due to orbital drifts of the NOAA  
 204 operational satellites. We have varied the local times such that from 2002 to 2014, they progress  
 205 from 12 to 18 hrs. Also shown is the corresponding 10.7 cm flux (black lines, right axis, units in  
 206 sfu). As can be seen, year 2002 was near solar maximum; the middle of solar cycle 23, and 2014  
 207 is some years into cycle 24, which began ~2008. The right panel (b) corresponds to the left  
 208 panel, but for temperature (K) at 45 km. The labels ‘CRC’ denote the correlation coefficients  
 209 between the respective ozone and temperature zonal means and the 10.7 cm flux.

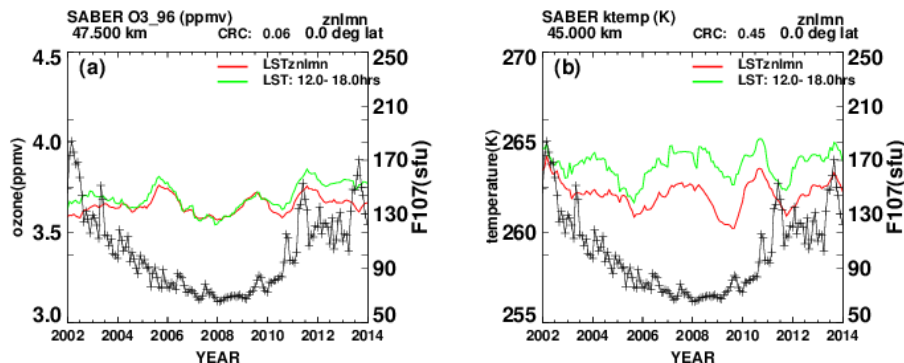
210 The estimates of responses to the solar cycle are made using Equation (1), in a similar manner  
 211 as previously done by others, and by us, using a multiple regression analysis (e.g., Keckut et al.  
 212 [2005], Soukharev and Hood [2006], Huang et al. [2016b]) that includes solar activity, trends,  
 213 seasonal, quasi biennial oscillations (QBO), and local time terms, among others, on monthly  
 214 values. Specifically, the estimates are found from the equation

$$215 M(t) = a + b * t + d * F107(t) + c * S(t) + l * lst(t) + g * QBO(t) \quad (1)$$

216 where  $t$  is time (months),  $a$  is a constant,  $b$  is the trend,  $d$  the coefficient for solar activity (10.7  
 217 cm flux),  $c$  is the coefficient for the seasonal ( $S(t)$ ) variations,  $l$  the coefficient for local time  
 218 variations, and  $g$  the coefficient for the QBO. As is often done, the seasonal and local time  
 219 variations are removed first, but we include them in Equation (1) for completeness. The F107  
 220 stands for the solar 10.7 cm flux, which is commonly used as a measure of solar activity, and the  
 221 values used here are monthly means provided by NOAA.  
 222

223  $M(t)$  stands for the input ozone or temperature zonal means described in a) and b), above.  
 224

225 The algorithm is applied to the monthly zonal-mean values from June 2002 through June 2014  
 226 (as in Figure 2), from 48°S to 48°N latitude, and from 20 to 100 km.  
 227



228  
 229 **Figure 2.** Ozone zonal mean mixing ratios (left panel, red line, ppmv) from mid 2002 to mid 2014, 47.5 km, 0° lat;  
 230 right panel, as in left panel, but for temperature (K) at 45km. Black lines (+, right scale) show the corresponding  
 231 monthly 10.7 cm flux (sfu) provided by NOAA.  
 232

### 233 3.0 Results: Ozone and temperature responses to solar cycle at 6, 18hrs (sunrise and sunset)

234 Specifically, we use the term ‘response to solar activity (solar cycle)’ generally to refer to the  
 235 term  $d * F107$  in Equation (1), and in particular to ozone or temperature responses at solar  
 236 maximum minus those at solar minimum, per 100 solar flux units (sfu). For ozone, it is also in



237 terms of percentage differences. A positive response means that the response at solar maximum  
238 is larger than that at solar minimum (Huang et al., 2016b).

239 For the new results of this study, we focus on the following:

- 240 1) Responses to the solar cycle at 6 and 18 hrs (sunrise, sunset). Comparisons with  
241 responses based on HALOE data (Beig et al. [2012], Fadnavis and Beig [2006]), which measure  
242 only at sunrise and sunset.  
243 2) Responses based on zonal means at specific local times.  
244 3) Responses with local times changing due to satellite orbital drifts.  
245 4) Comparison with results based on zonal means that are averages over both longitude and  
246 local time simultaneously, as in 3D models.

247

### 248 **3.1 Ozone responses at 6, 18hrs (sunrise and sunset)**

249 We consider first sunrise and sunset (6, 18hrs) because there are direct empirical results with  
250 which to compare, by Beig et al., [2012] and Fadnavis and Beig [2006], based on HALOE data  
251 from January 1992 to November 2005. Importantly, unlike other studies, they describe how they  
252 treat variations with local times, although they have results only at 6 and 18hrs.

253 The comparisons will indicate the quality of our results at 6 and 8hrs, and also over the 24 hrs  
254 of local time.

255 In Figure 3 and applicable other figures, we have manually transferred values of plots from  
256 other studies for comparison, so they are not exact, but should be adequate for our purposes.

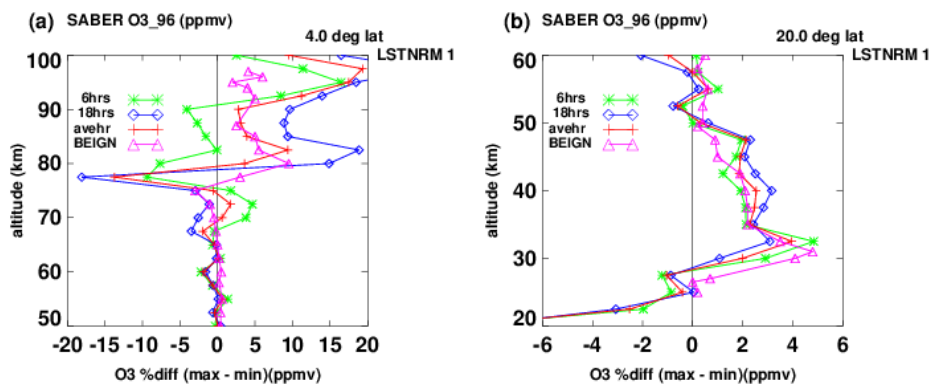
257 In comparisons with results based on HALOE data, uncertainties should be considered.  
258 According to Beig et al., [2012] and Fadnavis and Beig [2006], due to the sparse sampling  
259 inherent in solar occultation measurements, there are only 8 to 12 data points (sometimes less)  
260 per month for each latitude. So they generally present responses that are based on data  
261 composited over 30-degree latitude bins (e.g., 0-30°S, N) and averages of responses at sunrise  
262 and sunset. We get results at 4-degree intervals. Even if we composite the SABER data into 30°  
263 bins, the distribution within the bins would be uniform, but quite different than that of HALOE  
264 data, so we will present our results at specific latitudes. Our responses can vary significantly as a  
265 function of latitude, so that is another consideration in the comparisons.

266 In addition, here and in the literature, ozone responses are normally given in terms of percent  
267 changes, and the value of the ozone itself is needed to get percent values. Because absolute  
268 values among various instruments can sometimes be offset, it is an added source of uncertainty.

269 Figure 3 (left panel) shows our and that of Beig et al., [2012] ozone responses from 50 to 100  
270 km, at 4°N. The magenta triangles show responses based on HALOE data for ozone (composite,  
271 0-30°N, BEIGN), which are averages of sunrise and sunset responses, and should be compared  
272 with the red plusses, which denote the average of our results at 6hrs and 18hrs. It can be seen that  
273 the agreement of our averages (magenta triangles and red plusses) are very favorable, except for  
274 our large negative value at 77.5 km, and above 90km. As shown in Figure 4 (left panel), the  
275 results of Beig et al., [2012] for 6hrs and 0° also show a large negative value near 75 km. It is  
276 their values at 18 hrs (right panel) that seem anomalous (aside from what is shown in Figure 4,  
277 Beig et al., [2012] do not provide results separately for 6 and 18hrs). The green asterisks denote  
278 our results for 6hrs and the blue diamonds denote our responses at 18 hrs. The right panel  
279 corresponds to the left panel, but for 20°N and 20 to 60km, and the HALOE results are from  
280 Fadnavis and Beig [2006], 0-30°N composite. As in the left panel, the agreements of our  
281 averages (magenta triangles and red plusses) are very favorable. It can be seen that even in the  
282 stratosphere, the responses at 6hr are different from those at 18hrs.



283 Considering our discussion of uncertainties above, we believe that the results of Beig et al.  
 284 [2012] and Fadnavis and Beig [2006] (magenta triangles), agree very well with our estimates  
 285 (red plusses) in both altitude ranges (both panels of Figure 3). Note in particular the rapid change  
 286 from negative to positive values near 75-80 km. In Figure 3, the left panel at 4°N was chosen in  
 287 part to compare further with Figure 4, and the right panel at 20°N was chosen to compare with  
 288 Beig et al., [2012] results based on composite data in the 0-30° latitude band. We note that our  
 289 results show that there can be significant differences of responses at various latitudes.  
 290



291  
 292 **Figure 3.** Ozone responses to solar activity versus altitude, at 4°N, from 50 to 100 km (left panel), and 20°N, from  
 293 20 to 60km (right). Values are responses at solar max minus responses at solar min (% /100sfu). Magenta triangles  
 294 denote results by Beig et al. [2012], average of responses at 6 and 18 hrs local time, and 0-30°N. Red plusses  
 295 denote our estimate (average at 6 and 18 hrs). Green asterisks denote our estimate at 6hrs, and blue diamonds,  
 296 estimate at 18hrs.  
 297

298 Figure 4 shows ozone responses to solar activity versus altitude, from 50 to 100 km, at the  
 299 equator for sunrise (left) and sunset (right). Values are responses at solar max minus those at  
 300 solar min (% /100sfu). Red diamonds denote responses found by Beig et al. [2012] at 6 hrs (left  
 301 panel) and 18 hrs (right), composite from 0-4°N. Blue plusses denote our corresponding results  
 302 based on SABER data.

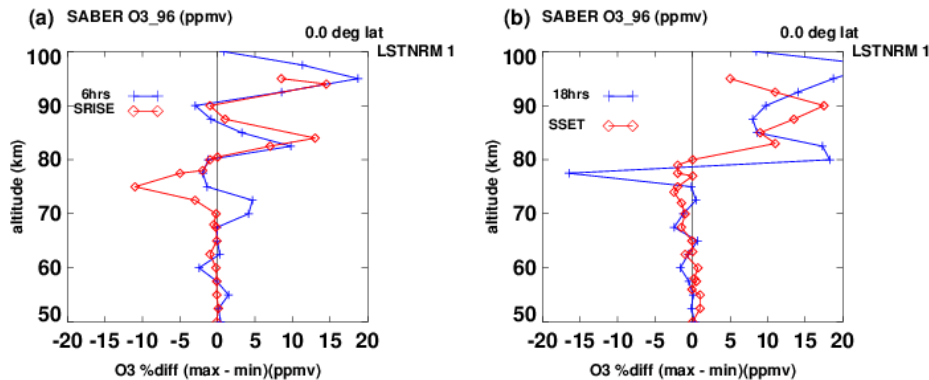
303 It is the only instance where Beig et al., [2012] show responses separately for 6 and 18hrs.

304 Except for the large negative values (red diamonds) from Beig et al [2012] in the left panel  
 305 near 74 km, and the large negative value (blue plusses) by us at 77.5 km in the right panel, we  
 306 believe that the comparisons are mostly favorable, in view of uncertainties discussed earlier.  
 307 Although not shown, the half width of the error bars provided by Beig et al., [2012] between 80  
 308 to 90 km are  $\sim \pm 10$  ((% /100sfu)

309 This can be compared with our results in the left panel of Figure 3 at 4°N. It is seen that  
 310 although there are sharp variations above 70km, the agreements are at least qualitatively good,  
 311 considering the caveats noted above.

312 The large excursions near 75 km are not isolated, but are systematic for both Beig et al.,  
 313 [2012] and us, as can be seen further in Figure 6 for 16°N.





314  
 315 **Figure 4.** Ozone responses to solar activity versus altitude, from 50 to 100 km, at the equator. Values are responses  
 316 at solar max minus responses at solar min (% /100sfu). Left panel: Red diamonds denote results by Beig et al.  
 317 [2012] at 6 hrs (left panel) and 18 hrs (right) local time, composite from 0-4°N. Blue plusses denote our results based  
 318 on SABER data at 6hrs and 0 deg (left panel) and 18hrs (right).  
 319

### 3.2 Results: Temperature responses at 6, 18hrs (sunrise and sunset)

320  
 321 Figure 5 corresponds to Figure 3, but for temperature. Values are responses at solar max minus  
 322 responses at solar min (°K /100sfu).

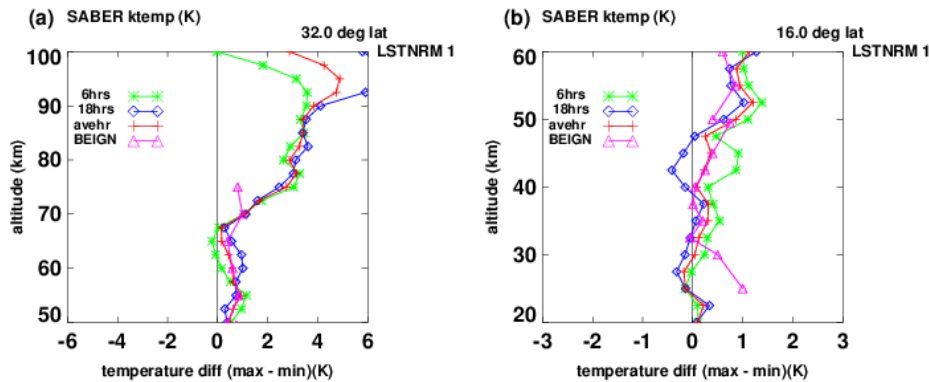
323 The left panel shows our and Beig et al.,[2012] temperature responses from 50 to 100 km, at  
 324 32°N. The magenta triangles show responses based on HALOE data, by Beig et al. [2012] for  
 325 temperature (composite, 0-30°N, BEIGN), which are averages of sunrise and sunset responses,  
 326 and should be compared with the red plusses which denote the average of our results at 6hrs and  
 327 18hrs. It can be seen that the agreement of our averages (magenta triangles and red plusses) are  
 328 very favorable, except at 75km. Beig et al.,[2012] do not provide temperature responses above  
 329 75 km. The green asterisks denote our results for 6hrs and the blue diamonds denote our  
 330 responses at 18 hrs. Beig et al.,[2012] do not provide results separately for 6 and 18hrs.

331 The right panel corresponds to the left panel, but at 16°N and 20 to 60km, and the HALOE  
 332 results are from Fadnavis and Beig [2006], 0-30°N composite. Above 30km, the agreements of  
 333 our averages (magenta triangles and red plusses) are very favorable. We note that according to  
 334 Fadnavis and Beig [2006] and Remsberg et al. [2002], that at altitudes below ~35km (~5hPa),  
 335 HALOE uses temperatures from the National Center for Environmental Prediction (NCEP).

336 This could be the reason for the differences between the magenta triangles and our red plusses  
 337 below 35 km.

338 It can be seen that even in the stratosphere, the responses at 6hr are different from those at  
 339 18hrs. We note that the left panel represents results at 32°N, instead of 16°N, as the agreement  
 340 with results by Beig et al. [2012] is somewhat better.

341  
 342



343  
 344  
 345  
 346  
 347  
 348  
 349  
 350

**Figure 5.** Corresponds to Figure 3, but for temperature responses to solar activity versus altitude, from 50 to 100 km (left panel), and 20 to 60 km (right). Values are responses at solar max minus responses at solar min  $^{\circ}\text{K}/100\text{sfu}$ . Magenta triangles denote results by Beig et al. [2012], averaged of 6 and 18 hrs local time (composite 0-30 $^{\circ}\text{N}$ ). Red plusses denote our estimate (average of 6 and 18 hrs, at 32 $^{\circ}\text{N}$  (left panel) and 16 $^{\circ}\text{N}$ , right panel), based on SABER data. Green asterisks denote our estimates at 6hrs, and blue diamonds are estimates at 18hrs.

#### 351 4.0 Ozone and temperature responses over a diurnal cycle.

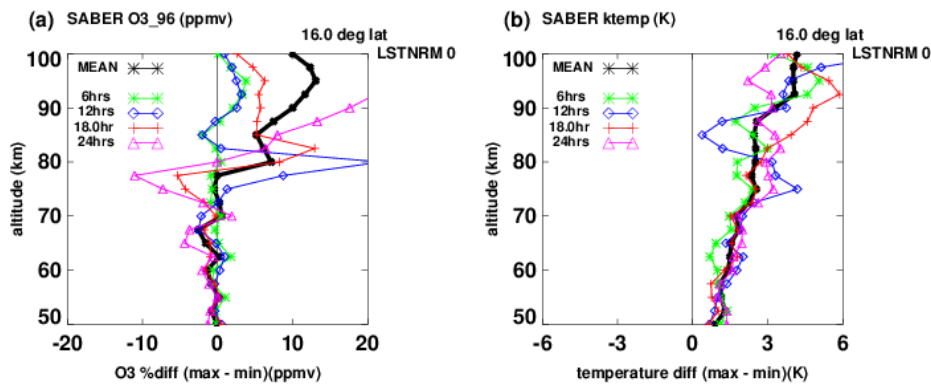
352 In this section, we extend our results to other local times.

353 Generally, previous studies based on other satellite measurements do not describe how they  
 354 treat data with respect to local times, and we cannot make comparisons as with HALOE.  
 355 Some studies use different data from various instruments, which mix data measured at different  
 356 local times. See Section 5.2 and the discussion in reference to Figure 9, for details.

357 Figure 6 shows our ozone (left panel) and temperature (right panel) responses from 50 to 100  
 358 km, at 16 $^{\circ}\text{N}$  over a diurnal cycle (6, 12, 18, 24hrs). The black line denotes our responses based  
 359 on SABER data where the zonal means are averages over both longitude and 24 hrs of local  
 360 time. The green asterisks denote responses for 6hrs, blue diamonds (12hrs), red plusses (18hrs),  
 361 and magenta triangles (24 hrs).

362 Up to this point, ozone values are responses at solar max minus responses at solar min  
 363 (percent/100sfu). In the following, note that unlike the situation above at 6 and 18hrs for ozone at  
 364 specific local times, the normalizing values used to obtain responses in percent are now averaged  
 365 over local time, to be consistent with responses based on zonal means that are averages over both  
 366 longitude and local time (black line in Figure 6).

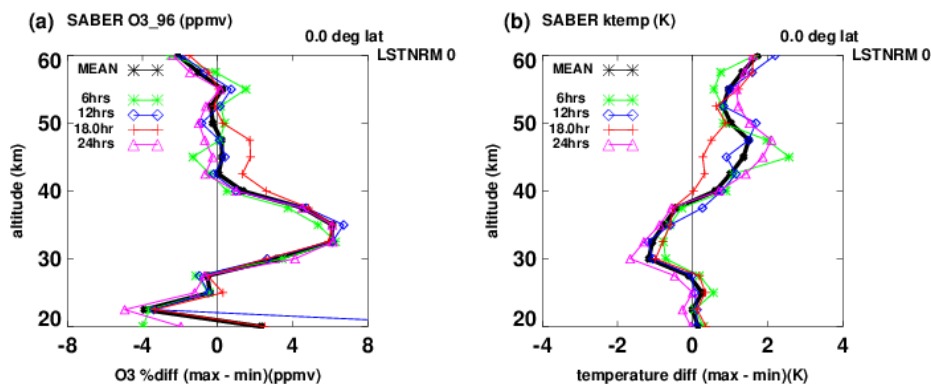
367



368  
 369 **Figure 6.** Ozone (left panel) and temperature (right) responses from 50 to 100 km at 16°N. Values are responses  
 370 at solar max minus responses at solar min (% /100sfu) for ozone and °K/100sfu for temperature. Black asterisks  
 371 denote responses based on zonal means that are averages over both longitude and local time. Green asterisks denote  
 372 our responses based on zonal means fixed at 6hrs, blue diamonds fixed at 12hrs, red plusses at 18 hrs, and magenta  
 373 triangles at 24hr, based on SABER data.

374  
 375 Figure 7 shows the ozone (left panel) and temperature (right panel) responses to solar activity  
 376 versus altitude, at the Equator, from 20 to 60 km, at 6hrs (green asterisks), 12hrs (blue  
 377 diamonds), 18hrs (red plusses), 24 hrs (magenta triangles), and based on zonal means that are  
 378 averages over local times (black asterisks). For ozone, below about 40 km, diurnal variations  
 379 have relatively little effect on responses. For temperature, the effects can be larger, even at  
 380 altitudes as low as 30 km.

381



382  
 383 **Figure 7.** As in Figure 6, but from 20 to 60 km. Ozone (left panel) and temperature (right) responses at 0°. Values are  
 384 responses at solar max minus responses at solar min (% /100sfu) for ozone and °K/100sfu for temperature. Black  
 385 asterisks denote our responses based on zonal means that are averages over both longitude and local time. Green  
 386 asterisks denote our responses of zonal means at 6hrs, blue diamonds at 12hrs, red plusses at 18 hrs, and magenta  
 387 triangles at 24hrs, based on SABER data.

388

389 **5.0 Comparisons with responses based on operational satellite measurements (fixed or**  
 390 **drifting local times).**



391 In the stratosphere and lower mesosphere, previous global results have been largely based on  
392 data from the NOAA operational satellites (including the Stratosphere Sounding Unit (SSU), the  
393 Microwave Sounding Unit (MSU), and the Solar Backscatter Ultraviolet (SBUV) instruments).  
394 An advantage of the operational satellites is that they can provide global measurements covering  
395 decades, being replaced as the instruments degrade. However, issues of calibration, instrument  
396 offsets, stability, and continuity, can be problematical. The satellites are generally polar orbiters  
397 and sun-synchronous, and make measurements at two fixed local times, one for the satellite  
398 ascending mode, and one for the descending mode.

399 As noted above, in merging data from different satellites, consistency in local times needs to  
400 be considered. Also, in some cases, over years, the orbits have drifted, so that the local times at  
401 which measurements are made have also drifted by several hours. See McPeters et al. [2013],  
402 Frith et al. [2014], Tummon et al. [2015], Hood et al., [2015]. Tumman et al. [2015] summarizes  
403 some of the data processing methods taken by various groups. Generally, they report that diurnal  
404 variations are either neglected, or are assumed to be negligible below  $\sim 45$ -50 km. See also Davis  
405 et al. (2015).

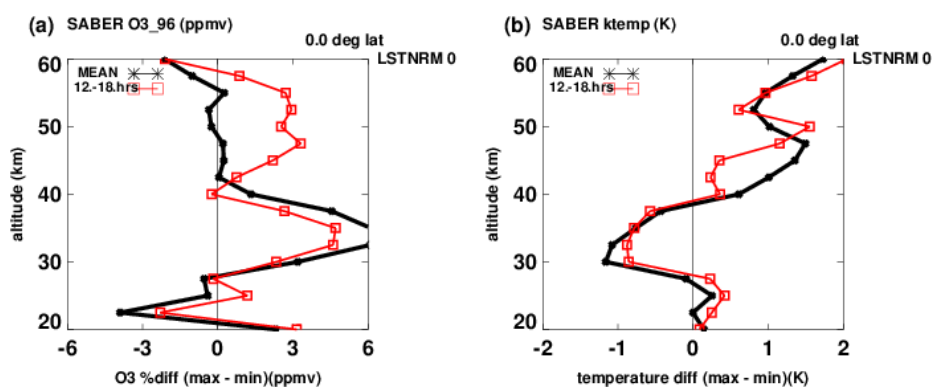
406 Unlike Beig et al.,[2012], the various studies generally did not address the issue of diurnal  
407 variations in detail.

408

#### 409 **5.1 Effects of local time variations due to satellite orbital drift**

410 To study the effects of local time changes due to orbital drift, from our estimates of diurnal  
411 variations, we can simulate their effects on responses to solar variability. As a simple example,  
412 Figure 8 shows our results for ozone (left panel) and temperature (right panel) responses to solar  
413 activity versus altitude, at the Equator, from 20 to 60 km. Values are responses at solar max  
414 minus responses at solar min in percent/100 sfu for ozone, and K/100 sfu for temperature. The  
415 red squares denote results where local times increased linearly from 12 to 18 hrs from 2002 to  
416 2014, to simulate orbital drift. Black asterisks denote responses based on zonal means that are  
417 averages over both longitude and local time. It can be seen that there are significant differences  
418 between them, especially above 40 km. We have also run tests with the local time varying at  
419 different hours and durations, and the differences can be smaller or more pronounced than that  
420 shown in Figure 8.

421



422

423

424

425

**Figure 8.** Ozone (left panel) and temperature (right panel) responses to solar activity versus altitude, at the Equator, from 20 to 60 km. Values are responses at solar max minus responses at solar min in % per 100 sfu for ozone, and K/100 sfu for temperature. Black asterisks denote responses based on zonal means that are averages over both



426 longitude and local time. Red squares denote corresponding results, but with local times increasing linearly from 12  
 427 to 18 hrs from 2002 to 2014.

428

429

## 5.2 Comparisons with operational satellite data

430

431

432

433

434

435

436

Figure 9 is taken from our previous analysis (Huang et al. [2016b], Figure 3). It compares results from previous studies done by others, which were manually transferred by us, so they are not exact. Our ozone responses (black line, SABER) are shown in the left plot (a), versus altitude from 20 to 60 km, averaged from 24°S to 24°N, to better conform to results by others. The light blue squares represent results of Remsburg (2008, RMSBRG), the green asterisks are from Fadnavis and Beig (2006, BEIGN, 0-30°N), and the blue diamonds are from Beig et al., (2012, BEIGS, 0-30°S), all based on HALOE data.

437

438

439

440

441

442

The red line (plusses) in Figure 9(a) show ozone responses from Soukharev and Hood [2006] (AUDTA, data from 1979-2003), as reported by Austin et al. [2008], and from models (AUMDL, magenta lines and triangles), also reported by Austin et al. [2008], representing composite results from 25°S to 25°N latitude. The Soukharev and Hood [2006] results (red plusses) are a composite based on SBUV, HALOE, and SAGE data, that show a minimum near 30 km, and a maximum above 40 km.

443

444

445

446

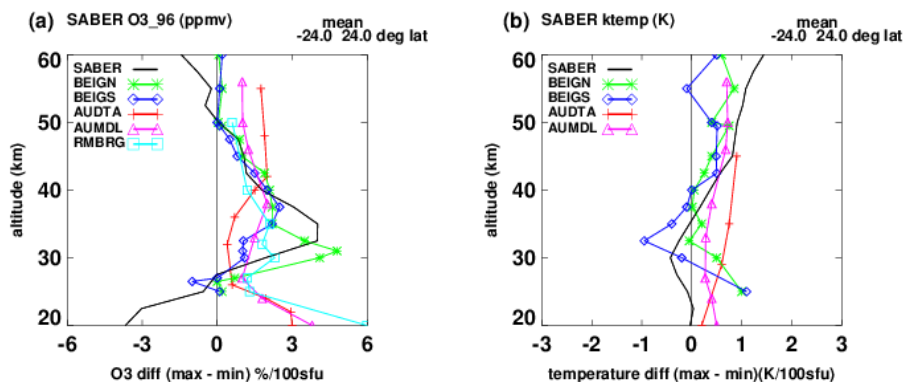
447

448

449

The right plot in Figure 9(b) corresponds to the left plot, but for temperature. The temperature responses (AUDTA, data from 1979-1997) were taken by Austin et al. [2008] from Scaife et al. [2000]. In Figure 9(b), the black line denotes our responses based on SABER data, averaged from 24°S to 24°N, to conform to previous results by others.

The issue of local time effects is not discussed in detail in these studies. As noted above, Austin et al., [2008] note that zonal means of models are averages over local time in contrast to those based on satellite measurements, which are typically at fixed local times.



450

451

452

453

454

455

456

**Figure 9.** Left panel (a): ozone responses versus altitude from 20 to 60 km; black line: SABER results averaged from 24°S to 24°N; light blue squares: Remsburg (2008, RMSBRG); green asterisks: Fadnavis and Beig, [2006], BEIGN, 0-30°N; blue diamonds :BEIGS, 0-30°S, HALOE data; red plusses: Austin et al. [2008] data AUDTA; magenta triangles, Austin et al., [2008] model, AUMDL, 25°S to 25°N latitude composite. Right panel (b): temperature responses corresponding to left panel.

457

458

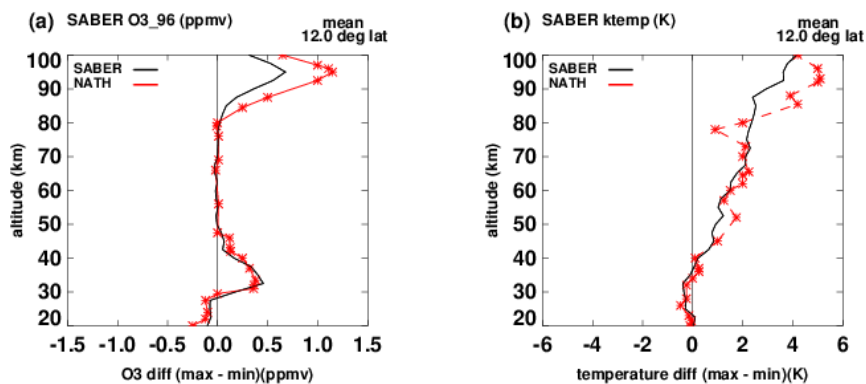
459

460

Nath and Sridharan [2014] have also analyzed the same SABER data as we did and derived responses at 10–15° latitude. Plots comparing with our results are given in Figure 10 (taken from Figure 5 of Huang et al. [2016a]). Black lines denote our results and red asterisks denote that by Nath and Sridharan [2014]. For both ozone and temperature, their responses agree better with



461 ours up to ~45km, but not so well at higher altitudes. We believe that the differences of the  
462 responses at higher altitudes are due to the local time variations in the SABER data, as discussed  
463 in Section 2. Nath and Sridharan (2014) do not appear to have considered diurnal variations.  
464 Note that in Figure 10 the ozone responses are not in percent differences, as in other plots, so that  
465 differences between 45 and 80 km are not readily discernible, due to their small values.  
466  
467

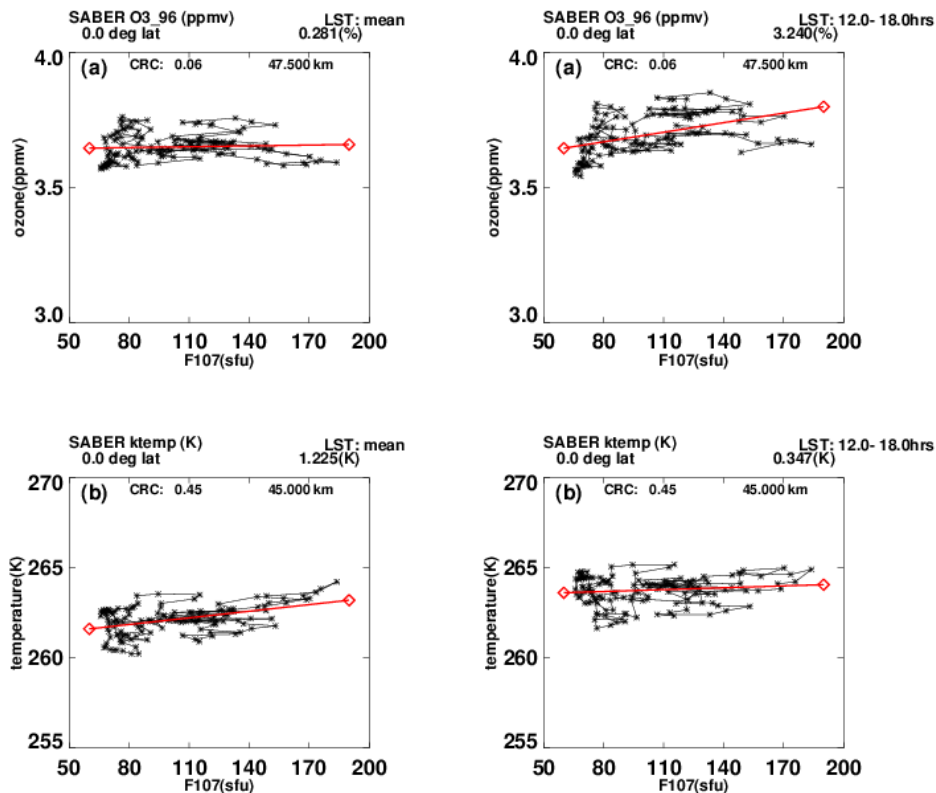


468  
469 **Figure 10.** Ozone (left) and temperature (right) responses to solar activity vs. altitude, from 20 to 100 km. Values  
470 are responses at solar max minus responses at solar min in ppmv/100 sfu for ozone and K/100 sfu for temperature.  
471 Black lines denote SABER responses at 12° lat; red color denotes results of Nath and Sridharan (2014), for 10–15°  
472 lat, also based on SABER data.  
473

#### 474 **6.0 Time span of measurements.**

475 Figure 11 is a scatter diagram plot of monthly values versus the 10.7 cm flux. The top row  
476 shows ozone at 47.5 km and the Equator, the bottom row shows temperature at 45 km and the  
477 Equator. The left panels represent the monthly zonal means that are averaged over both longitude  
478 and local time, and the right panels use zonal means where the local times simulate orbital drift  
479 as discussed in reference to Figure 8. The red lines in Figure 11 represent linear fits between the  
480 monthly values and the 10.7 cm flux, which corresponds to using only the solar term of the  
481 multiple regression (Eq. 1). For ozone (top row), the values 0.28 percent/100sfu (left header  
482 label, left panel) and 3.24 percent/100sfu at 47.5 km (right panel) compare well with the  
483 regression results which uses all terms of Eq. (1), seen in Figure 8 (left panel). For temperature  
484 (bottom row), the values 1.23K/100sfu and 0.35K/100sfu at 45 km also compare well with the  
485 right panel of Figure 8. Consequently, aliasing from other terms in Equation (1) is not  
486 significant. Unlike time series data, where time increases monotonically with data length, the  
487 10.7 cm flux values remain within a fixed interval between solar minimum and solar maximum  
488 (~70 and 200 sfu). In Fig. 11, the values span about one solar cycle. But even over more solar  
489 cycles, the 10.7 cm flux values would only repeat and backfill in with values in the same general  
490 area in Figure 11, effectively providing a more average result but not necessarily reducing the  
491 uncertainty much otherwise.

492 It can be argued that even with more than one solar cycle of data available, analysis over  
493 individual cycles should be made to analyze differences among solar cycles.  
494



495  
 496  
 497  
 498  
 499  
 500

**Figure 11.** Top row: scatter plot of ozone monthly values versus 10.7 cm flux (sfu) at 47.5 km and the Equator. Left (a): monthly values are zonal means, including average over local time. Right (b): as in (a), but zonal means include simulated local time variations of orbital drift. Bottom row: as in upper row, but for temperature monthly values. Red lines: linear fit between monthly values and 10.7 cm flux. Compare with Figure 8.

501  
 502  
 503  
 504  
 505  
 506  
 507  
 508  
 509  
 510  
 511  
 512  
 513  
 514  
 515  
 516  
 517

## 7.0 Summary and discussion.

Using SABER data, we have investigated the effects of ozone and temperature diurnal variations on their responses to the solar cycle, from 2002 to 2014, and 20 to 100 km.

We find that for ozone, above ~ 40km, zonal means reflecting specific local times (e.g., 6, 12, 18, 24 hrs) lead to different values of responses compared to each other, and compared to responses based on zonal means that are averaged over the 24 hours of local time (Figures 6,7). For temperature, effects of diurnal variations are not negligible at ~30 km and above.

We also have considered the variations of local times themselves due to orbital drifts of certain operational satellites, and their effects on responses to the solar cycle (Figure 8). The differences can be significant above ~35 km.

The quality and validity of our analysis are shown in comparisons with responses found by Beig et al., [2012], and Fadnavis and Beig, [2006], based on HALOE data, which made measurements only at sunrise and sunset. Comparisons with our corresponding results, based on SABER measurements, are favorable, both at sunrise and sunset separately, and combined. Our analysis is robust in that the average of responses at specific local times over a diurnal period of 24 hrs is the same as responses based on zonal means that are averages over longitude and local time together.



518 Previous studies based other satellite data generally do not describe their treatment, if any, of  
519 local times, so we cannot compare as for HALOE. Some studies also analyzed data merged from  
520 different sources, with measurements made at different local times. As discussed in Section 5.2  
521 in reference to Figure 9, the results of these studies do not generally agree very well among  
522 themselves.

523 We do not believe that diurnal variations are the major reason for the discrepancies, as there  
524 are likely other data-related issues. Other reasons for differences may be the conditions and  
525 constraints under which the various measurements were made (see Austin et al., 2008, Crooks  
526 and Gray [2005], Gray et al. [2005], Huang et al. [2016b])

527 However, diurnal variations should be included as part of the analysis of the differences  
528 among various results.

529 The effects due to satellite orbital drift (discussion in reference to Figure 8) may explain some  
530 unexpected variations in the responses, especially above 40 km.

531

#### 532 **Data availability**

533 The SABER data are freely available from the SABER project at <http://saber.gats-inc.com/>.

534

#### 535 **Acknowledgements.**

536

#### 537 **References**

538 Austin, J., Tourpali, K., Rozanov, E., Akiyoshi, H., Bekki, S., Bodeker, G., Bruhl, C.,  
539 Butchart, N., Chipperfield, M., Deushi, M., Fomichev, V. I., Giorgetta, M.A., Gray, L., Kadera,  
540 K., Lott, F., Manzini, E., Marsh, D., Matthes, K., Nagashima, T., Shibata, K., Stolarski, R. S.,  
541 Struthers, H., and Tian, W.: Coupled chemistry climate model simulations of the solar cycle in  
542 ozone and temperature, *J. Geophys. Res.*, 113, D11306, doi:10.1029/2007JD009391, 2008

543 Beig, G., Fadnavis, S., Schmidt, H., and Brasseur, G. P.: Inter-comparison of 11-year solar  
544 cycle response in mesospheric ozone and temperature obtained by HALOE satellite data and  
545 HAMMONIA model, *J. Geophys. Res.*, 117, D00P10, doi:10.1029/2011JD015697, 2012

546 Brasseur, G. P.: The response of the middle atmosphere to long term and short-term solar  
547 variability: A two-dimensional model, *J. Geophys. Res.*, 98, 23,079–23,090,  
548 doi:10.1029/93JD02406, 1993.

549 Brasseur, G. P. and Solomon, S.: *Aeronomy of the Middle Atmosphere*, Springer, Dordrecht,  
550 the Netherlands, 2005.

551 Chapman, S., and R. S. Lindzen (1970), *Atmospheric Tides*, Springer, New York.

552 Crooks, S. A. and Gray, L. J.: Characterization of the 11-year solar signal using multiple  
553 regression analysis of the ERA-40 dataset, *J. Clim.*, 18, 996–1015, 2005.

554 Davis, S. M., Karen H. Rosenlof, Birgit Hassler, Dale F. Hurst, William G. Read, Holger  
555 Vöme, Henry Selkirk, Masatomo Fujiwara, and Robert Damadeo, The Stratospheric Water and  
556 Ozone Satellite Homogenized (SWOOSH) database: a long-term database for climate studies,  
557 *Earth Syst. Sci. Data*, 8,461-490, 2016.

558 Fadnavis, S., and Beig, G.: Decadal solar effects on temperature and ozone in the tropical  
559 stratosphere, *Ann. Geophys.*, 24, 2091–2103, 2006.

560 Frith, S. M., Kramarova, N. A., Stolarski, R. S., McPeters, R. D., Bhartia, P. K., and Labow, G.  
561 J.: Recent changes in column ozone based on the SBUV version 8.6 merged ozone dataset, *J.*  
562 *Geophys. Res.-Atmos.*, 119, 9735–9751, doi:10.1002/2014JD021889, 2014.

563 Gille, S. T., A. Hauchecorne, and M.-L. Chanin (1991), Semidiurnal and





- 564 diurnal tidal effects in the middle atmosphere as seen by Rayleigh lidar,  
565 J. Geophys. Res., 96, 7579–7587.
- 566 Gray, L. J., Haigh, J. D., Harrison, R. G.: A Review of The Influence of Solar Changes on the  
567 Earth's Climate, Hadley Centre technical note 62, 1-81, 2005
- 568 Haigh, J.D., Austin, J., Butchart, N., Chanin, M-L., Crooks, S., Gray, L. J., Halenka, T.,  
569 Hampson, J., Hood, L. L., Isaksen, I.S.A., Keckhut, P., Labitzke, K., Langematz, U., Matthes, K.,  
570 Palmer, M., Rognerud, B., Tourpali, K., and Zerefos, C.: Solar variability and climate: selected  
571 results from the SOLICE project. *SPARC Newsletter No. 23*, 2004.
- 572 Hood, L. L., 2004: Effects of solar UV variability on the stratosphere. *Solar Variability and Its*  
573 *Effects on Climate, Geophys. Monogr.*, Vol. 141, Amer. Geophys. Union, 2004
- 574 Hood, L. L., Misios, S., Mitchell, D. M., Rozanov, E., Gray, L. J., Tourpali, K., Matthes, K.,  
575 Schmidt, H., Chiodo, G., Thiéblemont, R., Shindell, D., Krivolutsky, A., Solar Signals in CMIP-  
576 5 Simulations: The Ozone Response, *Quarterly Journal Royal Meteorological Soc.*, 141, 2670-  
577 2689, doi:10.1002/qj.2553, October, 2015
- 578 Huang, F. T., Mayr, H. G., Reber, C. A., Russell III, J. M., Mlynczak, M. G.: and Mengel, J.  
579 G.: Ozone quasi-biennial oscillations (QBO), semiannual oscillations (SAO), and correlations  
580 with temperature in the mesosphere, lower thermosphere, and stratosphere, based on  
581 measurements from SABER on TIMED and MLS on UARS, J. Geophys. Res., 113, A01316,  
582 doi:10.1029/2007JA012634, 2008a.
- 583 Huang, F. T., Mayr, H. G., Russell III, J.M., Mlynczak, M. G.: and Reber: C. A.: Ozone  
584 diurnal variations and mean profiles in the mesosphere, lower thermosphere, and stratosphere,  
585 based on measurements from SABER on TIMED, J. Geophys. Res., 113, A04307, doi:10.1029/  
586 2007JA012739, 2008b.
- 587 Huang, F. T., McPeters, R. D., Bhartia, P. K., Mayr, H. G., Frith, S. M., Russell III, J. M., and  
588 Mlynczak, M. G.: Temperature diurnal variations (migrating tides) in the stratosphere and lower  
589 mesosphere based on measurements from SABER on TIMED, J. Geophys. Res., 115, D16121,  
590 doi:10.1029/2009JD013698, 2010a.
- 591 Huang, F. T., Mayr, H. G., Russell III, J. M., and Mlynczak, M. G.: Ozone diurnal variations  
592 in the stratosphere and lower mesosphere, based on measurements from SABER on TIMED,  
593 J. Geophys. Res., 115, D24308, doi:10.1029/2010JD014484, 2010b.
- 594 Huang, F. T., Mayr, H. G., Russell III, J. M., and Mlynczak, M. G.: Ozone and temperature  
595 decadal trends in the stratosphere, mesosphere and lower thermosphere, based on measurements  
596 from SABER on TIMED, *Ann. Geophys.*, 32, 935–949, 2014.
- 597 Huang, F. T., Mayr, H. G., Russell III, J. M., and Mlynczak, M. G.: Ozone and temperature  
598 decadal responses to solar variability in the mesosphere and lower thermosphere, based on  
599 measurements from SABER on TIMED, *Ann. Geophys.*, 34, 29-40, doi:10.5194/angeo-34-129-  
600 2016a.
- 601 Huang, F. T., H. G. Mayr, J. M. Russell III, and M. G. Mlynczak, Ozone and temperature  
602 decadal responses to solar variability in the stratosphere and lower mesosphere, based on  
603 measurements from SABER on TIMED, *Ann. Geophys.*, 34, 801–813, doi:10.5194/angeo-34-  
604 801-2016, 2016b.
- 605 Keckhut, P., Cagnazzo, C., Chanin, M-L., Claud, C., Hauchecorne, A.: The 11-year solar-  
606 cycle effects on the temperature in the upper-stratosphere and mesosphere: Part I—Assessment  
607 of observations, *Journal of Atmospheric and Solar-Terrestrial Physics* 67, 940-947, 2005.
- 608 McPeters, R. D., Bhartia, P. K., Haffner, D., Labow, G. J., and Flynn, L.: The version 8.6  
609 SBUV ozone data record: An overview, *J. Geophys. Res.-Atmos.*, 118, 8032–8039,



- 610 doi:10.1002/jgrd.50597, 2013.
- 611 Nath, O., and Sridharan, S.: Long-term variabilities and tendencies in zonal mean TIMED–SABER  
612 ozone and temperature in the middle atmosphere at 10–15°N, *J. Atmos. Solar-Terr. Phys.*, 120, 1–8,  
613 2014.
- 614 Maycock, A., K. Matthes, S. Tegtmeier, R. Thiéblemont, and L. Hood, The representation of  
615 solar cycle signals in stratospheric ozone – Part 1: A comparison of satellite observations,  
616 *Atmos. Chem. Phys.*, doi:10.5194/acp-2015-882, 2016
- 617 Mitchell, D. M., L.J.Gray, M. Fujiwara, T. Hibino, J. A. Anstey, W. Ebisuzaki, Y. Harada, C.  
618 Long, S. Misios, P. A. Stott, and D. Tan, Signatures of naturally induced variability in the  
619 atmosphere using multiple reanalysis datasets, *Q. J. R. Meteorol. Soc.*, 141, 2011–2031,  
620 doi:10.1002/qj.2492, 2014.
- 621 Mukhtarov, P., Pancheva, D., and Andonov, B.: Global structure and seasonal and interannual  
622 variability of the migrating diurnal tide seen in the SABER/TIMED temperatures between 20  
623 and 120 km, *J. Geophys. Res.*, 114, A02309, doi:10.1029/2008JA013759, 2009.
- 624 Oberheide, J., M. E. Hagan, W. E. Ward, M. Riese, and D. Offermann (2000), Modeling the  
625 diurnal tide for the Cryogenic Infrared Spectrometers and Telescopes for the Atmosphere  
626 (CRISTA) 1 time period, *J. Geophys. Res.*, 105, 24,917–24,929.
- 627 Randel, W. J., Shine, K. P., Austin, J., Barnett, J., Claud, C., Gillett, N. P., Keckhut, P.,  
628 Langematz, U., Lin, R., Long, C., Mears, C., Miller, A., Nash, J., Seidel, D. J., Thompson, D. W.  
629 J., Wu, F., and Yoden, S., An update of observed stratospheric temperature trends, *J. Geophys.*,  
630 114, doi:10.1029/2008JD010421, 2009. Remsberg, E. E., Bhat, P. P., and Deaver, L. E.:  
631 Seasonal and long-term variations in middle atmosphere temperature from HALOE on UARS, *J.*  
632 *Geophys. Res.*, 107, D19, 4411,  
633 doi:10.1029/2001JD001366, 2002.
- 634 Remsberg, E. E.: On the response of Halogen Occultation Experiment (HALOE) stratospheric  
635 ozone and temperature to the 11-year solar cycle forcing *J. Geophys. Res.*, 113, D22304,  
636 doi:10.1029/2008JD010189, 2008
- 637 *J. Geophys. Res.*, 90, 5733–5743, 1985.
- 638 Russell, III J. M., Mlynczak, M. G., Gordley, L. L., Tansock, J., and Esplin, R.: An overview  
639 of the SABER experiment and preliminary calibration results, *Proceedings of the SPIE*, 44th  
640 Annual Meeting, Denver, Colorado, July 18–23, 3756, 277–288, 1999.
- 641 Sakazaki, T., Shiotani, M., Suzuki, M., Kinnison, D., Zawodny, J. M., McHugh, M., and  
642 Walker, K. A.: Sunset–sunrise difference in solar occultation ozone measurements (SAGE II,  
643 HALOE, and ACE-FTS) and its relationship to tidal vertical winds, *Atmos.*  
644 *Chem. Phys.*, 15, 829–843, doi:10.5194/acp-15-829-2015, 2015.
- 645 Shindell D, Rind, D., Balachandran, J., Lean, J., and Lonergran, P.: Solar cycle  
646 variability, ozone and climate. *Science*, 284, 305–308, 1999.
- 647 Scaife, A. A., J. Austin, N. Butchart, M. Keil, S. Pawson, J. Nash, and I. N.  
648 James (2000), Seasonal and interannual variability of the stratosphere diagnosed from UKMO  
649 TOVS analyses, *Q.J.R. Meteorol. Soc.*, 126, 2585–2604.
- 650 Soukharev, B. E., and L. L. Hood (2006), The solar cycle variation of stratospheric ozone:  
651 Multiple regression analysis of long-term satellite data sets and comparisons with models, *J.*  
652 *Geophys. Res.*, 111, D20314, doi:10.1029/2006JD007107.
- 653 Tummon, F., B. Hassler, N. R. P. Harris, J. Staehelin, W. Steinbrecht, J. Anderson, G. E.  
654 Bodeker, A. Bourassa, S. M. Davis, D. Degenstein, S. M. Frith, L. Froidevaux, E. Kyrölä, M.  
655 Laine, C. Long, A. A. Penckwitt, C. E. Sioris, K. H. Rosenlof, C. Roth, H.-J. Wang, and J. Wild,



656 Intercomparison of vertically resolved merged satellite ozone data sets: interannual variability  
657 and long-term trends, *Atmos. Chem. Phys.*, 15, 3021-3043, 2015  
658 Zeng, Z., W. Randel, S. Sokolovskiy, C. Deser, Y.-H. Kuo, M. Hagan, J. Du, and W. Ward  
659 (2008), Detection of migrating diurnal tide in the tropical upper troposphere and lower  
660 stratosphere using the Challenging Minisatellite Payload radio occultation data, *J. Geophys. Res.*,  
661 113, D03102, doi:10.1029/2007JD008725.  
662 Zhang, X., Forbes, J. M., Hagan, M. E., Russell III, J. M., Palo, S. E., Mertens, C. J., and  
663 Mlynczak, M. G.: Monthly tidal temperatures 20–120 km from TIMED/SABER, *J. Geophys.*  
664 *Res.*, 111, A10S08, doi:10.1029/2005JA011504, 2006.  
665